

IBA-JINR 400 MEV/U SUPERCONDUCTING CYCLOTRON FOR HADRON THERAPY

Y. Jongen, M. Abs, A. Blondin, W. Kleeven, S. Zarembo, D. Vandeplassche, IBA, Belgium
V. Aleksandrov, S. Gursky, O. Karamyshev, G. Karamysheva, N. Kazarinov, S. Kostromin,
N. Morozov, E. Samsonov, G. Shirkov, V. Shevtsov, E. Syresin, A. Tuzikov, JINR, Dubna, Russia

Abstract

The compact superconducting isochronous cyclotron C400 [[1, 2, 3, 4] has been designed by the IBA-JINR collaboration. It will be the first cyclotron in the world capable of delivering protons, carbon and α ions for cancer treatment. The cyclotron construction will start probably this year within the framework of the ARCHADE project [5] (Caen, France). $^{12}\text{C}^{6+}$ and $^4\text{He}^{2+}$ ions will be accelerated to 400 MeV/u and extracted by the electrostatic deflector. H_2^+ ions will be accelerated to the energy of 265 MeV/u and extracted by stripping. The magnet yoke has a diameter of 6.6 m; the total weight of the magnet is about 700 t. The designed magnetic fields are 4.5 T and 2.45 T respectively in the hills and in the valleys. Superconducting coils will be enclosed in a cryostat. All other parts and subsystems of the cyclotron will be warm. Three external ion sources will be mounted on the switching magnet on the axial injection line located below the cyclotron.

The main parameters of the cyclotron, its design, the current status of the development work on the cyclotron systems are presented.

INTRODUCTION

Today, cancer is the second highest cause of death in industrial countries. Its treatment still presents a real challenge. Protons and light ions allow depositing the radiation dose more precisely in a cancer tumor, reducing greatly the amount of dose received by healthy tissue surrounding the tumor as compared with electrons. But in addition to the ballistic accuracy of protons, light ion beams, like carbon beams, have an extra advantage in radiation therapy: they have a different biological interaction with cells and are very effective even against some type of cancerous cells which resist usual radiations. That is why in the last years an increasing interest in the particle therapy based on $^{12}\text{C}^{6+}$ ions has been seen.

IBA, the world's industrial leader in equipment of the proton therapy centers, and the team of accelerator physicists from JINR have developed a superconducting C400 cyclotron based on the design of the current proton therapy C235 cyclotron.

BASIC CONCEPT OF CYCLOTRON

Most of the operating parameters of the C400 cyclotron are fixed: fixed final kinetic energy, fixed magnetic field and fixed RF system frequency (small main magnetic field and RF frequency changes are necessary to switch

between different accelerated ions). The cyclotron is relatively small and cost effective.

The most important parameters of the 400 MeV/u superconducting cyclotron are listed in Table 1. The view of the cyclotron is presented in Fig.1.

Table 1: Main parameters of the C400 cyclotron

General properties	
accelerated particles	H_2^+ , $^4\text{He}^{2+}(\alpha)$, $(^6\text{Li}^{3+})$, $(^{10}\text{B}^{5+})$, $^{12}\text{C}^{6+}$
injection energy	25 keV/Z
final energy of ions, protons	400 MeV/u 265 MeV/u
extraction efficiency	~70 % (by deflector)
number of turns	~2000
Magnetic system	
total weight	700 t
outer diameter	6.6 m
height	3.4 m
pole radius	1.87 m
valley depth	0.6 m
bending limit	K = 1600
hill field	4.5 T
valley field	2.45 T
RF system	
number of cavities	2
operating frequency	75 MHz, 4 th harmonic
radial dimension	1.87 m
vertical dimension	1.16 m
dee voltage:	
center	80 kV
extraction	160 kV

Three external ion sources are mounted on the switching magnet on the axial injection line located below the cyclotron. $^{12}\text{C}^{6+}$ ions are produced by a high-performance ECR at current 3 μA , α particles and H_2^+ ions are also produced by a simpler ECR source. All species have a charge to mass q/m ratio of 1/2 and all ions

are extracted at the same voltage 25 kV, so the small retuning of the RF system frequency and a very small magnetic field change achieved by different excitation of 2 parts of the main coil are needed to switch from H_2^+ to α or to $^{12}C^{6+}$ ions. The expected time to switch between species will be no longer than two minutes, like the time needed to retune the beam transport line between different treatment rooms.

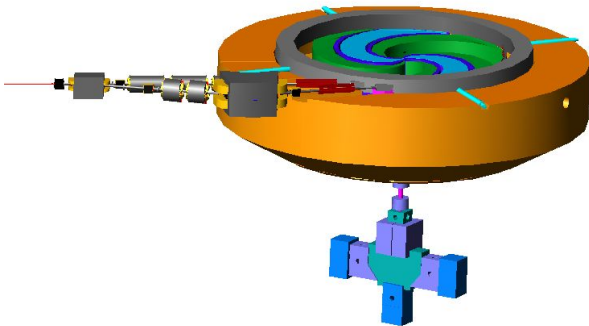


Figure 1: View of the median plane in the C400 superconducting cyclotron

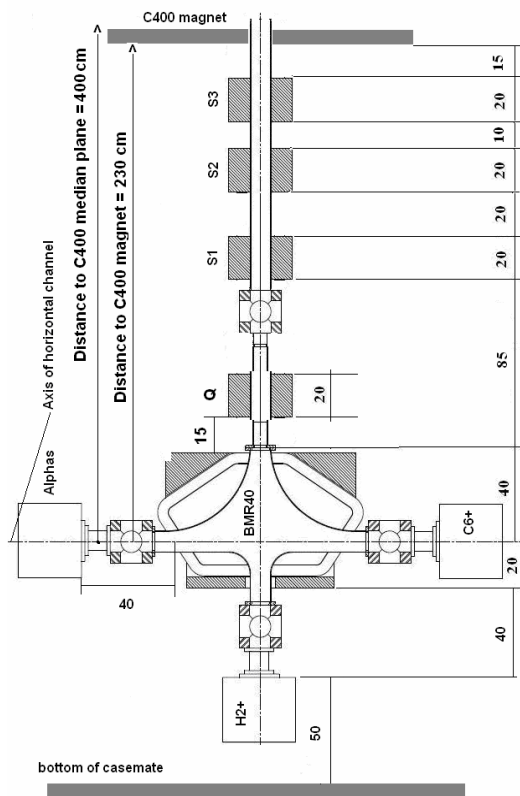


Figure 2: Scheme of the injection beam line

Focusing in the axial injection channel (Fig.2) is provided by three solenoid lenses (S1, S2, S3), the rotational symmetry of the beam is reestablished with the help of the quadrupole Q placed immediately downstream the dipole bending magnet BMR40. This 90° bending magnet has two horizontal and one vertical entrances and the common exit for all ion beams. The bending radius of

the BMR40 magnet is 400 mm. The maximum magnetic field is 0.075 T and the gap height is 70 mm. The maximum magnetic field of the solenoids is below 0.3 T, a good field region is 80 mm. The maximum quadrupole lens gradient is below 10 mT/cm.

The main feature of the axial injection system is the presence of the strong stray magnetic field not only in the vertical part of the channel but also in its horizontal part. For this reason, ion sources, the switching magnet and the quadrupole of the axial injection beam line have to be shielded. Beam transport line calculations indicate that for all types of ions the beam diameter at the spiral inflector entrance is smaller than 2 mm.

A model of the dee tip geometry at the cyclotron center with the inflector placed inside the housing was developed (see Fig. 3). Dee tips have the vertical aperture 12 mm in the first turn and 20 mm in the second and further turns. On the first turn the gaps were delimited with pillars reducing the transit time. The azimuthal extension between the centers of the accelerating gaps was chosen to be 45°. The electric field in the inflector was chosen to be 20 kV/cm. Thus, the height (electric radius) of the inflector is 2.5 cm. The gap between the electrodes is 6 mm, and the tilt parameter $k'=0.1$. To reduce the fringing field effects, the aspect ratio of the electrode width to the gap between electrodes is 2. The electric potential distribution simulation of the central region was performed.

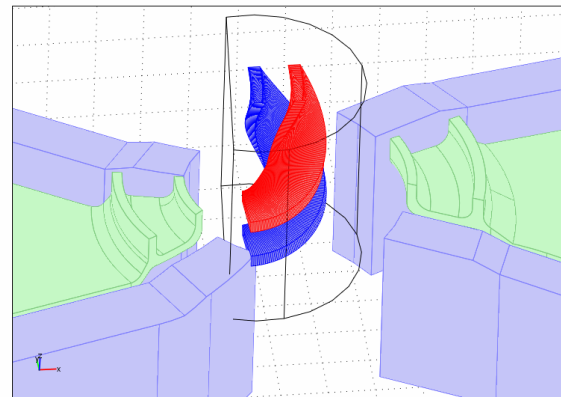


Figure 3: Central region with the spiral inflector model

The magnetic field bump (about 200 G) in the central region does not provide sufficient magnetic axial focusing. The electric axial focusing plays the main role during first turns.

Beam simulations has shown that using two phase selection slits, the injection efficiency is about 12% for ions with amplitudes of radial oscillations smaller than 4 mm. The use of the buncher will increase the beam intensity at least by a factor of two.

The possibility of modulating the beam intensity by changing voltage of inflector electrodes was tested. Particles have been tracked through the inflector with decreasing voltage. It is necessary to decrease voltage by about 12% to lock the beam. Results indicate that this

method of intensity modulation has one disadvantage – radial displacement of the beam – but it is smaller than 1 mm.

MAGNETIC SYSTEM

The simulation and design of the C400 magnetic system was based on its main characteristics: four-fold symmetry and spiral sectors; the deep-valley concept with RF cavities placed in the valleys; the elliptical pole gap is 120 mm at the center decreasing to 12 mm at extraction; magnetic induction inside the yoke is below 2.2 T; the main coil current is 1.2 MA. An elliptical gap between the spiral sectors provides stable beam acceleration up to 10 mm from the pole edge. Keeping the last orbit as close as possible to the pole edge facilitates extraction. The main parameters of the cyclotron magnetic system were optimized by computer simulation using the well known Vector Fields OPERA-3D software package.

The view of the magnet with spiral sectors is given in Fig. 4. The sectors have the following parameters: the initial spiral parameter $N\lambda=77$ cm with increasing spiral angle to the final radius with the parameter $N\lambda\sim 55$ cm; the sector azimuthal length varies from 25° at the cyclotron center to 45° at the sector outer edge; the axial profile is an ellipse with the 60 and 1874-mm semi-axes. At large radii the axial profile of the ellipse is cut by planes at the distance $z=\pm 6$ mm from the median plane.

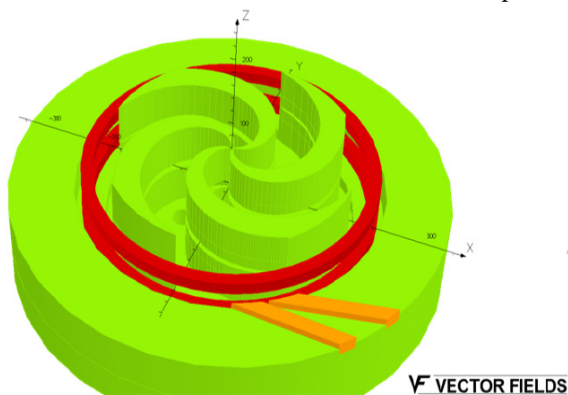


Figure 4: OPERA-3D simulation of the C400 magnetic system

The average magnetic field and amplitudes of the basic number Fourier harmonics as a function of radius are shown in Fig. 5. The required isochronous magnetic field was shaped by profiling the azimuthal length of sectors. The accuracy of the average magnetic field at the shaping simulation is ± 10 G in the middle and end regions of the beam acceleration. The optimized sector geometry provides axial betatron oscillation frequency (vertical tune) $Q_v\sim 0.4$ in the extraction region (see Fig. 6) to decrease the vertical beam size and to minimize effects of field imperfections.

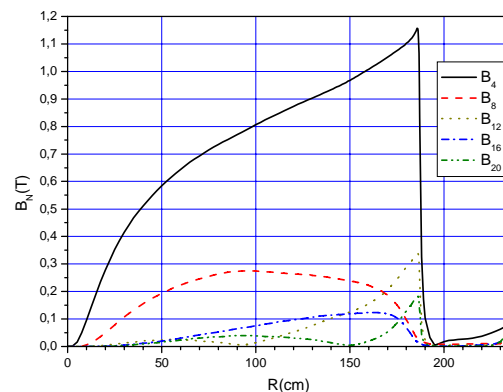
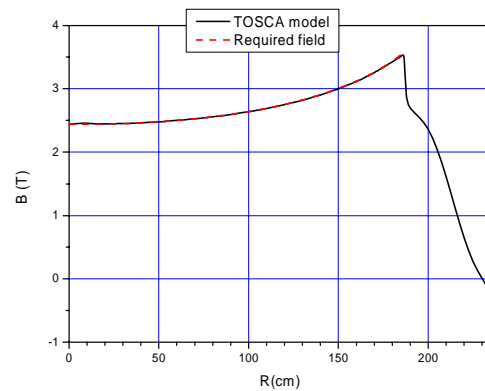


Figure 5: Up: average magnetic field; down: amplitudes of Fourier harmonics of the cyclotron magnetic field as a function of radius

During the magnet simulation the following design goals were achieved:

- Optimization of the magnet sizes
- Avoiding dangerous resonances
- Realization of the vertical tune $Q_z \sim 0.4$ in the extraction region
- Keeping the optimal value of the spiral angle of the sectors (minimize total sector phase angle change)
- Average magnetic field shaping by variation of the sector azimuth width
- Last orbit kept as close to the pole edge as possible (~ 10 mm)
- Minimization of iron weight, keeping the stray field at an acceptable level
- Optimal solution for the SC coil design
- Optimal design solution for the trimming of the magnetic field change from carbon to H_2^+ ions :
 - a) RF frequency change by 0.6%,
 - b) main coil consisting of two parts,
 - c) excitation current redistribution in two parts of the main coils by means of additional small current (60 A) power supply.

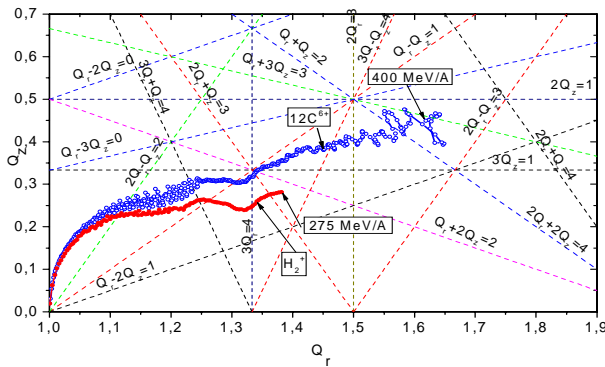


Figure 6: Working diagram of the cyclotron

ACCELERATING SYSTEM

Acceleration of the beam will occur at the fourth harmonic of the orbital frequency, i.e. at 75 MHz, and will be obtained through two normal conducting cavities [6] placed in the opposite valleys.

The geometric model of the double-gap delta cavity housed inside the valley of the magnetic system of the C400 cyclotron was developed in the CST Microwave Studio [7]. The finally chosen geometry is presented in Fig.7. The depth of the valley permits using the cavity with the total height 1160 mm. The vertical aperture of the dee was 20 mm. The accelerating gap width was 6 mm in the center increasing to 80 mm at radius R=750 mm and remaining constant up to the extraction region .

Cavities have a spiral shape complementary to the shape of the sectors. The sector geometry permits azimuthal extension of the cavity (between the middles of the accelerating gaps) equal to 45° up to the radius of 1500 mm then decreasing to 32° in the extraction region. Four stems were inserted with different transversal dimensions in the model. Different positions of the stems were studied to insure increasing voltage along the radius of the accelerating gap, which should range from 80 kV in the central area to 160 kV in the extraction region. It is important to have a high value of the voltage approximately from the radius R=1500 mm before the crossing of the resonance 3Q_r=4.

Thickness of the dee was 20 mm. The edges of the dees were 10 mm thick and have a rounded form.

Calculations of the created model were performed using the eigenmode JD lossfree solver (Jacobi Division Method) in the CST MICROWAVE STUDIO and the Block LANCZOS solver in ANSYS. The half-structure model of the cavity was used where the vertical symmetry is presented.

Shaping of the radial voltage distribution is obtained by adjustment of stems positions. The variation of the horizontal dimensions of all stems by one percent changes the frequency by about 300 kHz. The value of the voltage along the radius does not change noticeably while the frequency is shifted less than 1 MHz.

Simulations show that the frequencies from both codes are similar when the number of mesh cells is 7 millions for CST and 3 millions for ANSYS:

F_{rf} =75.02 MHz, CST Microwave Studio
 F_{rf} =74.80 MHz, ANSYS

The accuracy of the calculations for the cavity frequency is better than 0.3%. One can see in Fig. 8 that the difference between the acceleration gap voltage profiles in two codes is negligible.

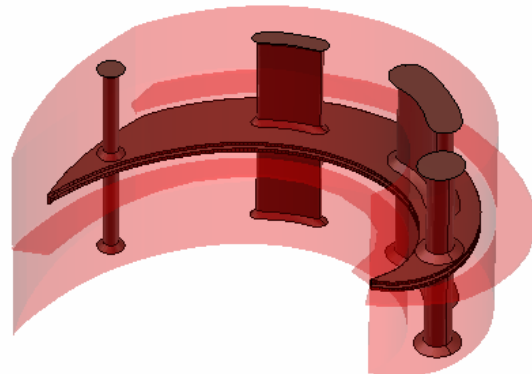


Figure 7: View of the cavity model

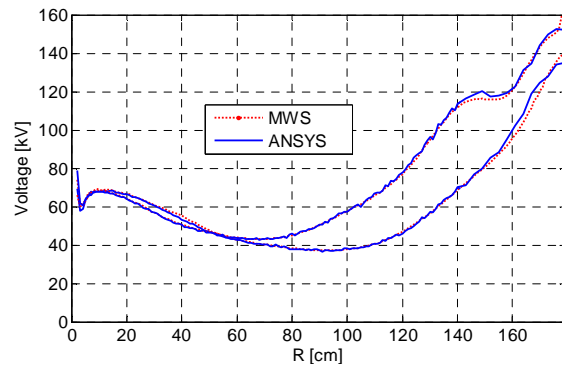


Figure 8: Voltage distribution along radius on both sides of dees calculated using two independent methods

Power dissipation in the model was calculated with the assumption that the wall material is the copper with conductivity $\sigma=5.8 \cdot 10^7$ 1/($\Omega \cdot m$). The quality factor was about 14000 and power losses of the model were as follows:

For the stored energy 1 J the voltage in the center is 65 kV and the average losses are 35 kW.

For the stored energy 1.5 J the voltage in the center is 80 kV and the average losses are about 50 kW.

Each cavity will be powered by a 75 MHz, 100 kW tetrode-based amplifier (as used in the current C235). The cavities will be excited with the RF generator through a coupling loop (which should be rotated azimuthally within small limits (± 30 degrees)). The active tuning system must be designed to bring the cavities to the frequency initially to compensate for detuning because of temperature variations due to RF heating and to provide frequency difference 450 kHz for $^{12}C^{6+}$ and H_2^+ ions acceleration. It was found that the best position for the tuner is at the radius R=1200 mm (between the second and third stems).

It was demonstrated that it was possible to fit the resonant frequency of the cavity by varying diameter of

the fourth stem. The frequency difference per diameter difference is about 100 kHz/mm.

ION DYNAMICS

Detailed beam dynamics simulations were performed to be sure that the resonances crossed during acceleration would not cause significant harmful effect to the beam. During a whole range of acceleration the carbon beam crosses the lines of 15 resonances up to 4th order (Table 2). The working diagrams presented in Fig. 6 were computed via the analysis [8] of small oscillations around the closed orbits. All resonances can be subdivided into two groups. The first group consists of 6 internal resonances ($nQ_r \pm kQ_z = 4$, $n, k=0, 1, 2, 3, 4, n+k \leq 4$) having the main 4th harmonic of the magnetic field as a driving term. The second group includes 11 external resonances ($nQ_r \pm kQ_z = m$, $m=0, 1, 2, 3$) that could be excited by the magnetic field perturbations.

The analysis of dangerous resonances defines limits of acceptable magnetic field imperfections. All these limits can be achieved in practice.

Table 2: List of resonances up to 4th order

Resonance, (Level of danger)	Radius (cm) (Driving Term)	Description, tolerances
$Q_r = 1$ (Yes)	2-10 (B_{z1})	Increase in radial amplitudes $B_{z1} < 2-3$ G
$4Q_r = 4$ (Not)	2-10 (B_{z4}, φ_{z4})	Weak influence on radial motion at acceleration
$2Q_r - Q_z = 2$ (Not)	110 (B_{z2}, B_{r2})	Increase in axial amplitudes $B_{z2} < 200$ G, $B_{r2} < 50$ G
$3Q_r + Q_z = 4$ (Not)	131 (B_{z4}, φ_{z4})	No influence up to $A_z, A_r = 5-7$ mm
$Q_r - Q_z = 1$ (Yes)	145 (B_{r1})	Increase in axial amplitudes $B_{r1} < 5-7$ G
$3Q_r = 4$ (Yes)	154 (B_{z4}, φ_{z4})	Increase in radial amplitudes beginning with $A_r = 1.5$ mm. Can be corrected by average field perturbation.
$2Q_r + Q_z = 3$ (Not)	157 (B_{r3})	Increase in axial amplitudes $B_{r3} < 10$ G
$Q_r + 2Q_z = 2$ (Not)	162 (B_{z2})	Increase in axial amplitudes $B_{z2} < 20$ G
$3Q_z = 1$ (Not)	167 (B_{r1})	Increase in axial amplitudes $B_{r1} < 20$ G
$3Q_r - Q_z = 4$ (Not)	167 (B_{z4}, φ_{z4})	Increase in radial amplitudes. No

		influence if no axial amplitudes increase on resonance $3Q_z = 1$ due to B_{r1} .
$2Q_r = 3$ (Not)	172 (B_{z3})	Increase in radial amplitudes. $B_{z3} < 10$ G
$Q_r + Q_z = 2$ (Not)	177 (B_{z2}, B_{r2})	Increase in radial and axial amplitudes. $B_{r2} < 10$ G
$2Q_r + 2Q_z = 4$ (Not)	177 (B_{z4}, φ_{z4})	No influence
$Q_r + 3Q_z = 3$ (Not)	179 (B_{z3})	Increase in axial amplitudes $B_{z3} < 10$ G
$2Q_r - Q_z = 3$ (Not)	180 (B_{z3})	Increase in axial amplitudes $B_{z3} < 10$ G
$2Q_r + Q_z = 4$ (Not)	181 (B_{z4}, φ_{z4})	Increase in axial amplitudes. Requires proper deflector positioning.
$2Q_z = 1$ (Yes)	181 (B_{z1}, B_{r1})	Increase in axial amplitudes. $B_{r1} < 10$ G, $dB_{z1}/dr < 1$ G/cm

EXTRACTION

Extraction of protons will be done by means of the stripping foil. It was found that 320 MeV is the possible minimum kinetic energy of protons that can be extracted during one turn downstream the stripping foil passage and 265 MeV is the minimum energy of protons for 2-turn extraction (Fig. 9). The second solution was chosen because the energy of extracted protons is closer to the usually applied energy for the proton beam treatment. The stripper foil is at the radius of 1634 mm, the azimuth is 56° in the chosen coordinate system.

Electrostatic deflection extraction will be used for carbon and α beam. The single electrostatic deflector located in the valley between the sectors will be used with the electric field about 150 kV/cm. The extraction efficiency was estimated about 73% for the septum with increased (0.1 - 2) mm thickness along its length. The extraction of the carbon and proton beams by the separate channels and their further alignment by the bending magnets outside the cyclotron was chosen as the acceptable solution. A plan view of both extraction beam lines is shown in Fig. 10. The passive magnetic elements (correctors) will be used inside the cyclotron and the active elements (quadrupole lenses and bending magnets) outside the yoke. The system for carbon ion extraction consists of the electrostatic deflector, two passive magnetic correctors MC1-2, three quadrupole lenses CQL1-3 and two steering dipole magnets CSM1-2. The proton beam extraction system consists of the stripping foil, magnetic corrector PMC1, two bending magnets BM1-2, two quads PQL1-2 and two steering magnets PSM1-2.

Both beams have a spot with $\sigma_{x,y} < 1$ mm at the degrader entrance, located 675 cm from the cyclotron

center.. Transverse emittances are $(10\pi \text{ mm}\cdot\text{mrad}, 4\pi \text{ mm}\cdot\text{mrad})$ and $(3\pi \text{ mm}\cdot\text{mrad}, 1\pi \text{ mm}\cdot\text{mrad})$ for the extracted carbon and proton beams, respectively.

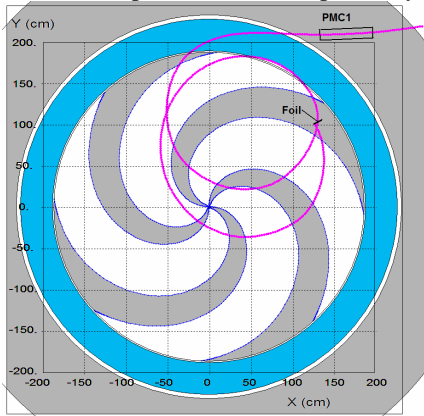


Figure 9: Two-turn extraction of protons with energy 265 MeV

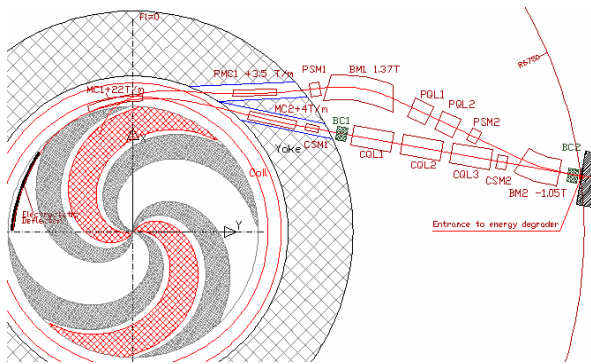


Figure 10: Layout of the C400 cyclotron with two extraction lines

VACUUM REQUIREMENTS

Numerical simulations of the beam transmission efficiency dependent on the charge exchange of H_2^+ and C^{6+} ions with the residual gas have been carried out for the future cyclotron. The loss of the beam intensity due to collision breakup with the residual gas molecules is determined by the cross sections for the losses process over a wide energy range and depends on the pressure distribution. A uniform pressure in the cyclotron was assumed because external injection is used. Nitrogen was assumed as a residual gas.

Different methods were used for cross section estimation for H_2^+ and C^{6+} ions. Losses in the axial injection line were estimated from experimental data on cross sections for the fixed projectile energy. The theoretical approach crosschecked by some experimental data for given energies was used for cyclotron vacuum chamber volume.

Vacuum requirements in the injection line are determined by $^{12}\text{C}^{6+}$ ions and beam losses are about 2 % for the pressure $2 \cdot 10^{-7}$ torr.

Losses of H_2^+ ions during acceleration due to electron stripping were estimated using Bohr's formula [9].

The vacuum requirements in the cyclotron are determined by H_2^+ ions. For the pressure the 10^{-7} torr estimated losses will be 2-5 %; for the pressure $2 \cdot 10^{-7}$ torr, 4-10 %. Losses of C^{6+} ions will not exceed 1% for the pressure $2 \cdot 10^{-7}$ torr.

CONCLUSIONS

Computer modeling of the main systems and detailed simulations of the beam dynamics in the C400 cyclotron have been performed.

The results show that the energy range up to 400 MeV/amu ($K = 1600$) can be achieved with the compact design similar to that of the existing IBA C235 cyclotron. Transmission of carbon ion beam between the ion source and the beam extraction foil was estimated as 13%.

The C400 cyclotron will also provide a proton therapy beam with energy 265 MeV. Losses of protons due to the charge exchange with the residual gas during acceleration will not exceed 10% and extraction will be without losses.

Design of different cyclotron subsystems is presently in progress.

REFERENCES

- [1] Y. Jongen et al., "Design studies of the compact superconducting cyclotron for hadron therapy", X EPAC 06, Edinburg, Scotland, 2006.
- [2] Yves Jongen et al, "IBA C400 Cyclotron Project for Hadron Therapy", The 18th International Conference on Cyclotrons and their Applications Cyclotrons 2007, Laboratori Nazionali del Sud, Giardini Naxos, Italy 2007.
- [3] Y.Jongen at al, "Current status of the IBA C400 cyclotron project for hadron therapy", XI EPAC08, p.1806-1809, Italy, 2008.
- [4] Y.Jongen at al, "Simulation and design of the compact superconducting cyclotron C400 for hadron therapy", Proc. 11 Internal Heavy Ion Accelerator Technology, D9, Italy, 2009.
- [5] <http://archade.fr/>.
- [6] Yves Jongen et al, "Radio Frequency System of the Cyclotron C400 for Hadron Therapy", The 18th International Conference on Cyclotrons and their Applications Cyclotrons 2007, Laboratori Nazionali del Sud, Giardini Naxos, Italy 2007. <http://felino.elettra.trieste.it/cyc07/papers/TUPPRA05.pdf>.
- [7] CST STUDIO SUITE <http://www.cst.com>.
- [8] Y. Jongen et al., "Numerical study of the resonances in superconducting cyclotron C400", in Proc. of Cyclotrons 2007, p. 382.
- [9] Franzke B. "Interaction of stored beams with the residual gas".